CrossMark

ARTICLE

Microstructural evolution, mechanical profile, and fracture morphology of aluminum matrix composites containing graphene nanoplatelets

Mahmood Khan, Maham Amjad, and Ansa Khan
Composite Research Centre, Department of Materials Science and Engineering, Institute of Space Technology, Islamabad 44000, Pakistan

Rafi Ud-Din
Materials Division, Pakistan Institute of Nuclear Science and Technology, Nilore 45650, Pakistan

Iftikhar Ahmad
Deanship of Scientific Research, Advanced Manufacturing Institute, King Saud University, Riyadh 11421, Kingdom of Saudi Arabia

Tayyab Subhani[a)]
Composite Research Centre, Department of Materials Science and Engineering, Institute of Space Technology, Islamabad 44000, Pakistan

(Received 9 January 2017; accepted 13 March 2017)

Aluminum matrix composites were prepared by powder processing route containing three different loadings of graphene nanoplatelets, i.e., 1 wt%, 3 wt%, and 5 wt%. Ball milling of composite powders was performed to ensure the uniform dispersion of nanoplatelets in aluminum powder, followed by their consolidation to near theoretical densities. Microstructural evolution after composite preparation was witnessed by X-ray diffraction, optical microscopy, and scanning electron microscopy, while the mechanical property profile was evaluated by hardness, compression, and flexural tests. The mechanical properties of composites containing 5 wt% nanoplatelets were found with maximum improvements in hardness, compression, and flexural strengths of 35%, 433%, and 283%, respectively. This increase in mechanical performance is related to uniform dispersion and microstructural development in composites by incorporating nanoplatelets. Fractographic characterization indicated a change in fracture morphology from matrix-dominant in pure aluminum to nanoplatelet-dominant in composites. In particular, shearing and pull out of nanoplatelets were observed during the fracture of composites with simultaneous restricted plastic deformation of the surrounding aluminum matrix.

I. INTRODUCTION

Aluminum matrix composites (AMCs) are widely used for aerospace and automobile applications due to their attractive mechanical properties.[1] As a result, a variety of fibers and particles have been reinforced in aluminum and its alloys including metallic carbides,[2] oxides,[3] borides,[4] and nitrides.[5] Among reinforcements, carbon fibers have been extensively incorporated in AMCs due to their increased strength and stiffness.[6] The recently emerged carbon-based nanomaterials, i.e., carbon nanotubes (CNTs) and graphene nanoplatelets (GNPs) are considered to provide better mechanical properties than their micrometer-sized cousins, i.e., carbon and graphite fibers.[7] Therefore, CNTs and GNPs are highly attractive to prepare a novel class of composites containing carbonaceous reinforcements at nanometer scale and initial investigations have provided promising results.[8,9] However, the real translation of mechanical properties of CNTs and GNPs into nanocomposites has not yet been achieved. The issues related to the dispersion of CNTs and GNPs in the aluminum matrix, their consolidation to near theoretical densities, and in particular the control on the reinforcement–matrix interface are still unaddressed. In comparison to CNT-reinforced AMCs, GNP-reinforced AMCs have been less studied and demand thorough investigation so that the effect of these two-dimensional nanoreinforcements could be explored after incorporating in a metallic matrix.

Generally, powder processing technique[10] is used to prepare graphene nanoplatelet reinforced aluminum matrix composites (GNP-AMCs). GNPs are mixed with aluminum powder and milled to prepare a composite powder, which is later densified by pressureless[11] and pressure-assisted[12] techniques. The understanding of the incorporation of nanoplatelets of graphene in aluminum

Contributing Editor: Jürgen Eckert
[a)]Address all correspondence to this author.
e-mail: tayyab.subhani@ist.edu.pk
DOI: 10.1557/jmr.2017.111

 © Materials Research Society 2017

https://doi.org/10.1557/jmr.2017.111 Published online by Cambridge University Press

particles along with the densification of the composite powders into a solid body is required. The mechanisms providing mechanical strength and stiffness of these nanocomposites under the concept of stress transfer from the matrix to the reinforcement and the role of the interface are the other significant topics to be addressed. Moreover, the extent of improvement in mechanical properties by the addition of GNPs together with microstructural evolution demands an in-depth investigation. Finally, the deformation mechanism and fracture morphology in ductile matrix composites containing GNPs is another area still unexplored. The deformation mechanism in composites is difficult than in a pure matrix without any reinforcement. In particular, the incorporation of GNPs having high strength and modulus along with flexible nature may produce a new deformation mechanism after incorporating in a ductile matrix, which may be different from the composites containing ceramic reinforcements. In addition, the shearing mechanism in GNPs due to weak van der Waals forces between graphene layers along with their wrinkled morphology may introduce a novel fracture behavior after incorporating in a ductile matrix.

In the present study, GNPs were incorporated in pure aluminum to produce composites with three different GNP loadings. The aim is to introduce GNPs in high contents, i.e., up to 5 wt% to investigate their effect on the microstructural and mechanical properties of the composites, so as to develop composites for futuristic requirements. Finally, a critical review of the data on a similar topic was presented and the results obtained were discussed in the light of the available literature.

II. EXPERIMENTAL

A. Materials

Gas atomized aluminum powder with a purity level of 99.5% was used in the present work [Fig. 1(a)]. Aluminum powder had spherical morphology with attached satellite particles. GNPs were produced by Hummers' method using fine graphite flakes as the starting material [Fig. 1(b)]. The diameter of GNPs was 5–20 μm with thickness of >10 nm. The particle size of as-received aluminum powder was evaluated using a laser diffraction particle size analyzer (Mastersizer 3000, Malvern Instruments, Malvern, United Kingdom), as given in Fig. 1(c).

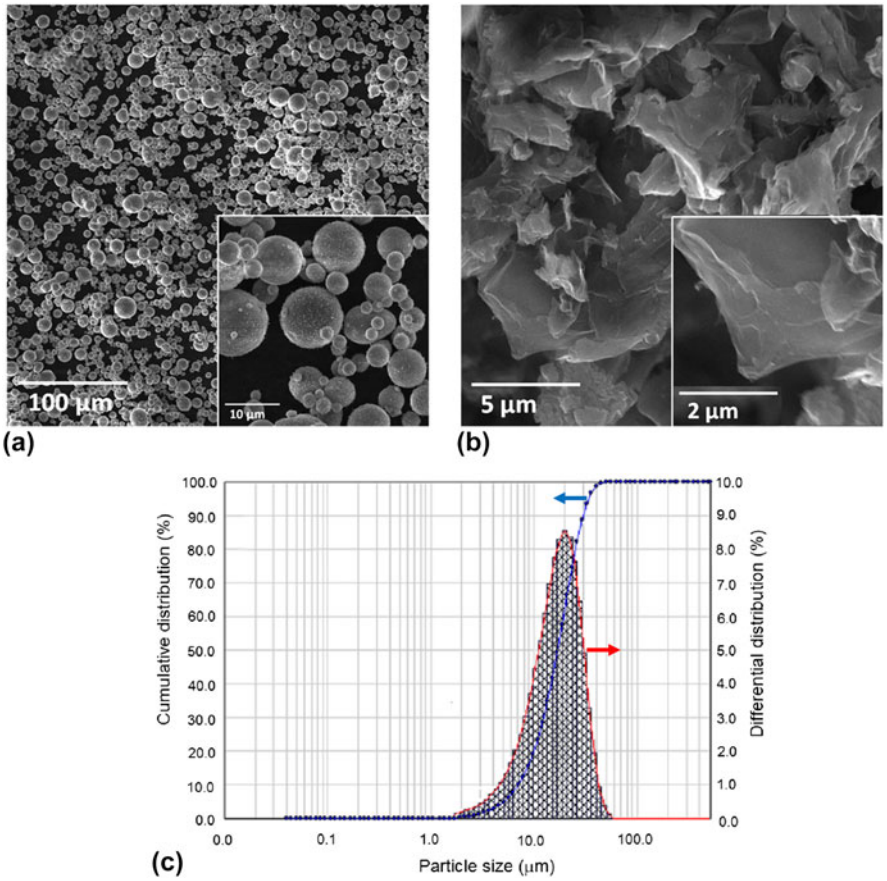


FIG. 1. SEM images of as-received (a) pure aluminum powder and (b) GNPs used in the present study to prepare composites; insets are the images at high magnification. (c) Particle size analysis of pure aluminum powder used in the present study showing average particle size and cumulative and differential distributions.

https://doi.org/10.1557/jmr.2017.111 Published online by Cambridge University Press

B. Manufacturing

GNPs in required quantity were dispersed in acetone and ultrasonicated for 2 h at a frequency of 24 kHz using a probe sonicator (Hielscher UP400S, Hielscher Ultrasonic GmbH, Teltow, Germany). Aluminum powder was added to the suspension of GNPs and sonicated for 1 h. The suspension was later filtered and dried at 90 °C for 4 h in a vacuum oven (Model EQ-DZF-6020, MTI Corporation, Richmond, California). The dried composite powder was sealed in a stainless steel vessel of diameter 25 mm and height 70 mm and milled in a milling machine (Model RZ-04149-05, Cole-Parmer Instrument Company, Vernon Hills, Illinois). Zirconia balls were used as grinding media in a ratio of 10:1, while milling was performed at 350 rpm for 2 h. After mechanical milling, the composite mixture was placed in a clean and dried vial and properly sealed to avoid the absorption of moisture and the inclusion of contamination. The schematic of the complete composite processing is shown in Fig. 2.

For consolidation, the composite powder in required quantity was filled in a steel die of inner cavity of 20 mm and cold compacted in a hydraulic press (Specac Hydraulic Press, Specac Limited, Kent, United Kingdom) under a pressure of 125 MPa. The prepared composite green bodies were sintered in a tube furnace (KJ-1600 G, Zhengzhou Kejia Furnace Company, Henan, China) under argon atmosphere. The heating rate was 5 °C/min, while heating temperature and holding time were 600 °C and 6 h, respectively, followed by furnace cooling.

Following the same route, three types of aluminum matrix composites containing 1, 3, and 5 wt% GNPs were prepared along with a reference sample of aluminum by following the same manufacturing route. The sintered composite pellets were later used for the characterization of physical, microstructural, and mechanical properties.

C. Characterization

The densities of the sintered composites were measured using the buoyancy method (Archimedes principle). A densimeter (AU-900S, DongGuan HongTuo Instrument Company, Guangdong, China) was used with an accuracy of 10^{-3} g. Optical microscopy was performed using an optical microscope (Metkon IMM 901, Metkon Instruments, Inc., Bursa Turkey) at magnifications up to 400×. Grinding and polishing were carried out on a grinding/polishing machine (Metkon Forcipol 2V, Metkon Instruments Inc.). Silicon carbide emery papers of grit sizes 600, 800, 1200, 1600, and 2000 were used at rotational speeds of 130–220 rpm. The polishing was performed using an alumina paste of particle sizes of 20 and 5 μm to obtain scratch-free and mirror-like surface. The polishing process was followed by etching the specimens with a Keller's reagent (190 mL distilled water with 5 mL HNO_3, 2 mL HF, and 3 mL HCl) with an immersion time of 30 s.

Scanning electron microscopy (SEM) of the composites was performed on a microscope (MIRA-III, FEG-SEM, Tescan Orsay Holding, Brno, Czech Republic). SEM images were acquired in the secondary electron imaging mode at an accelerating voltage of 10 kV. The composite specimens were attached on the aluminum stubs with carbon tape. The fracture surfaces of reference and composite specimens were also observed under SEM to investigate the fracture morphology. Energy dispersive spectroscopy (EDS) was performed on a spectrometer (X-MaxN Silicon Drift Detector, Oxford Instruments, Abingdon, United Kingdom) attached with a microscope. X-ray diffraction (XRD) of sintered composites was performed to identify the phases in composite specimens. XRD was performed in the 2θ range of 10°–80° on an X-ray diffractometer (X-ray Bruker D8, Bruker Corporation, Billerica, Massachusetts) using Cu K_α radiation.

The hardness of the composites was performed using a Vickers hardness tester (HV-50A, DongGuan Sinowon Precision Instrument Co Ltd., DongGuan, China). Hardness tests were performed by applying the indenter load of 5 kg for the dwelling time of 10 s. At least five values of each composite specimen were acquired to obtain an average hardness value. The hardness was measured on the surface of specimens parallel to the applied uniaxial load during cold pressing. Compression testing was performed on a tensile testing machine (WDW-30, Jinan Testing Equipment IE Corporation, Jinan, China). The strain rate used for the testing of specimens of dimensions 12 × 6 × 6 mm was 0.2 mm/min, while at least five tests of each composite were performed. Flexural strength was performed on the same

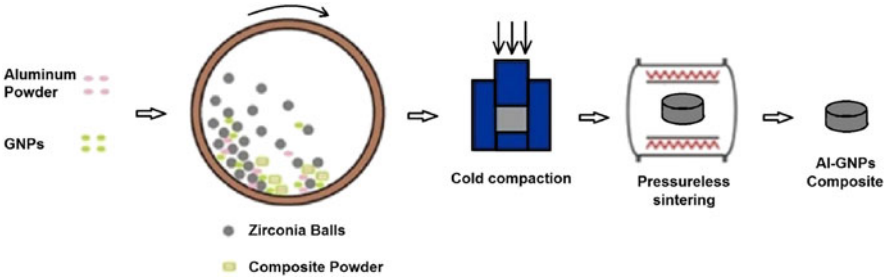


FIG. 2. Schematic of manufacturing aluminum matrix composites containing GNPs; ball milling, cold compaction, and consolidation by pressureless sintering are shown.

https://doi.org/10.1557/jmr.2017.111 Published online by Cambridge University Press

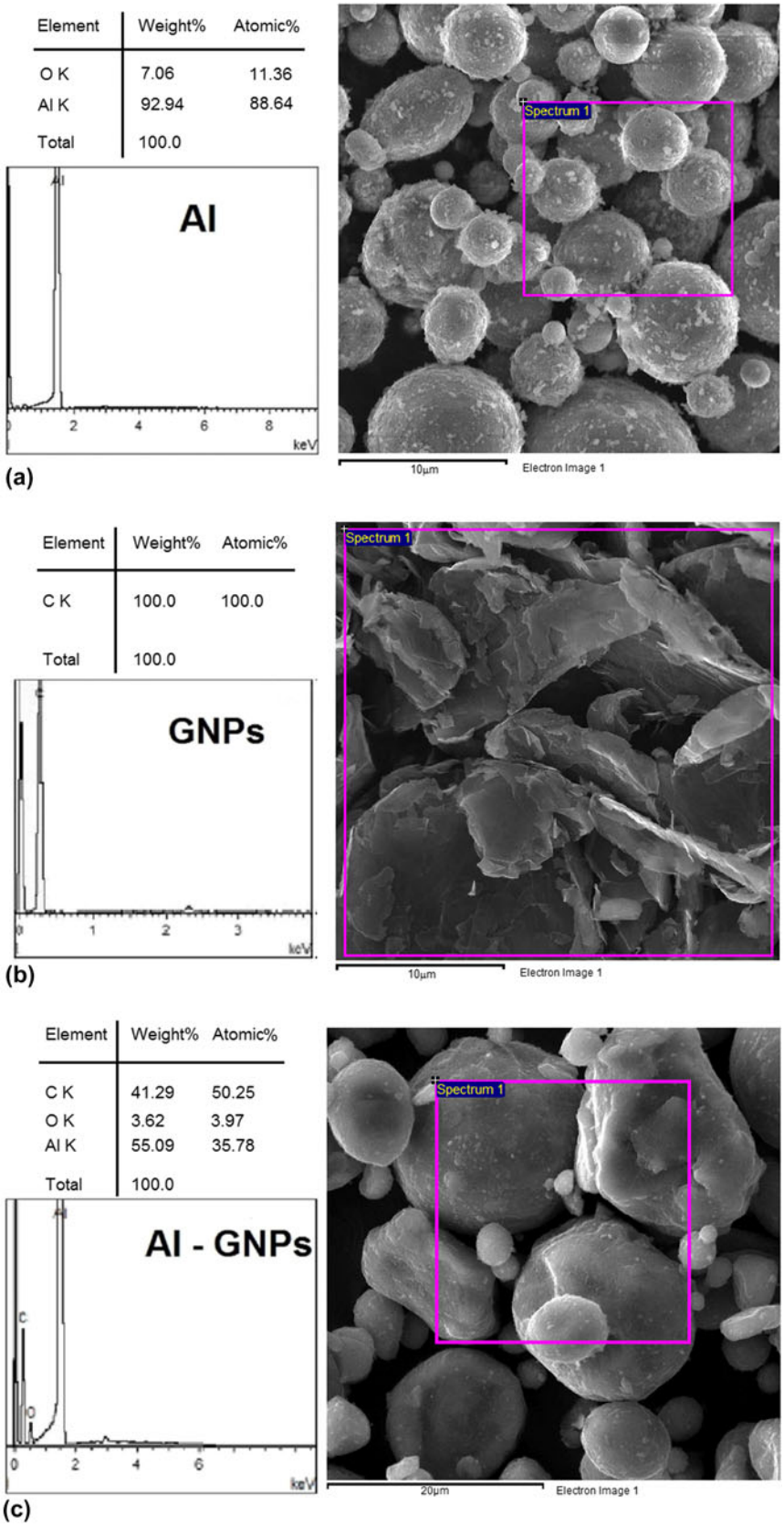


FIG. 3. EDS results of (a) pure aluminum powder, (b) GNPs, and (c) composite powder of aluminum containing 3 wt% GNPs; the presence of carbon on aluminum particles indicates that graphene layers have been attached to aluminum powder.

https://doi.org/10.1557/jmr.2017.111 Published online by Cambridge University Press

tensile testing machine; the samples were cut using a low speed cutter (Buehler Isomet, ITW Company, Lake Bluff, Illinois) in dimensions of 20 × 8 × 4 mm.

III. RESULTS AND DISCUSSION

A. Composite powder

The results of EDS analysis of pure aluminum, GNPs, and composite powders are shown in Fig. 3; the presence of oxygen in aluminum powder has been detected, which may be due to the formation of oxide at the surface of particles. Figures 4(a) and 4(b) show the presence of GNPs in aluminum powder before ball milling. It can be seen that after ball milling, the layers of GNPs have been deposited on aluminum powder after shearing action [Figs. 4(c) and 4(d)]. Moreover, fine aluminum particles have been embedded in GNPs [Figs. 4(e) and 4(f)]. The plastic deformation of aluminum powder has also been

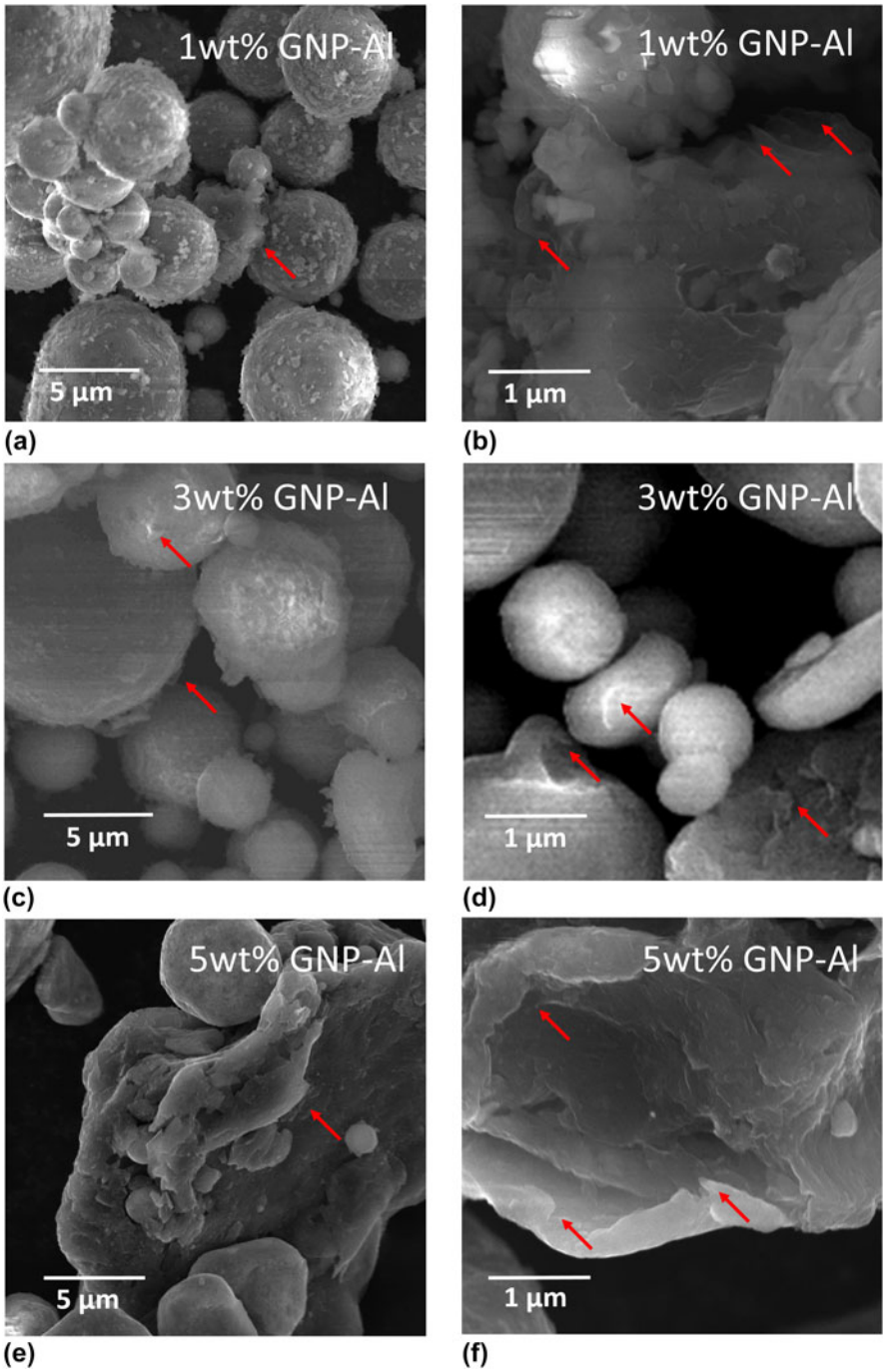


FIG. 4. SEM images of aluminum powder after ball milling; (a and b) 1 wt% GNPs in aluminum powder, (c and d) 3 wt% GNPs in aluminum powder, and (e and f) 5 wt% GNPs in aluminum powder.

https://doi.org/10.1557/jmr.2017.111 Published online by Cambridge University Press

observed after milling action and their complete spherical morphology has been disturbed.

B. Microstructure

Figures 5(a), 5(c), 5(e), and 5(g) show the optical micrographs of composites and pure aluminum at two different magnifications. All the images were taken with similar digital imaging contrast. The microstructures at low magnification show the densification of composites without the indication of any significant porosity. The microstructures at high magnification reveal the bonding of aluminum powders after sintering while the particles and prior particle surfaces are also visible. Fractional pores can also be viewed in microstructures conforming the relative densities of the composites, as discussed earlier. GNPs cannot be identified at these magnifications under light microscopy.

SEM micrographs of pure aluminum and composites are shown in Figs. 5(b), 5(d), 5(f) and 5(h). No significant porosity can be seen in the images and the detectable contents match the densities of the composites. Moreover, there was no indication of the presence of GNP-agglomerates at the magnifications under observation. A further increase in the magnification on fracture composite surfaces revealed the presence of GNPs, as observed and discussed further below.

C. X-ray diffraction

XRD patterns of pure aluminum and composites are plotted in Fig. 6. Typical peaks corresponding to aluminum can be seen, while any peak corresponding to GNPs could not appear except in the composite containing 5 wt% GNPs.[13] The same GNP peaks in a ceramic matrix have also been reported.[14,15] A possible reason may be the detection limit of the equipment, which could not resolve the presence of GNPs in composites containing 1 and 3 wt% GNPs, as also observed elsewhere.[16,17] Also the peaks corresponding to the presence of aluminum carbide (Al_4C_3) did not appear.[18] Again, either the quantity of Al_4C_3 was insufficient to be resolved by an XRD machine or aluminum did not react with GNPs to form Al_4C_3. The involvement of pressure along with temperature in pressure-assisted sintering techniques such as hot-pressing may aid the formation of Al_4C_3 along the GNP/Al interface.[19] The presence of XRD peaks in 5 wt% GNP–Al samples can be attributed to their presence as GNP-clusters, also visible in Figs. 4(e) and 4(f). These clusters may have been detected in XRD. However, in 1 wt% GNP–Al and 3 wt% GNP–Al composites, no such presence was detected and graphene sheets after shearing were mixed with aluminum powder.

D. Density

The density values of sintered composites are presented in Table I; theoretical and experimental densities found by buoyancy method along with relative densities are given. To calculate the theoretical densities of the composites by the rule of mixtures, the densities of the two constituents of composites, i.e., aluminum and GNPs were taken to be 2.7 g/cm^3 and 1.8 g/cm^3, respectively. Being lighter than aluminum, GNPs reduce the density of composites though the significant reduction in the density of composites comes after incorporating large volumes of GNPs. The relative densities were calculated using theoretical densities and experimental densities. Figure 7(a) plots the relative densities of the composites and pure aluminum. It can be seen that pure aluminum showed the highest relative density of ~99%, which is in good agreement with the literature value.[17] Generally, the incorporation of reinforcement in composites decreases their density.[20] A similar observation was noted in the current study that the incorporation of GNPs reduced the density of composites and the trend continued with a systematic increase in their loading fractions. Considering the fact that pressureless sintering was used without the employment of a secondary processing technique, such as rolling or forging, the measured densities in this investigation are comparable with the literature values[21] and are at a level to explore the incorporating effect of GNPs on microstructural and mechanical properties. The decrease in relative density is due to factors like porosity[22,23] and clustering of the reinforcement.[24] The presence of GNP-clusters was found in composites containing 5 wt% GNPs, which was responsible for the presence of porosity and decrease in the relative density of the composites. The evidences of the presence of clusters may be witnessed in Figs. 4(e) and 4(f), which also show the cluster encapsulating the smaller aluminum particles. These clusters cause the decrease in the density of composites and the effects appear significantly at higher values of GNPs. Large differences in the melting point of the two constituents, i.e., GNPs: ~4625 °C and aluminum: 660 °C, which provide less tendency to make bonds between the two composites constituents, also leads to a higher porosity content.[23]

E. Hardness

The hardness values of pure aluminum and composites are plotted in Fig. 7(b). Pure aluminum has a value of 22 ± 3 HV, which increased to 25 ± 2 HV by adding 1 wt% GNPs showing 15% increase in hardness. Further rises in the contents of GNPs to 3 wt% and 5 wt% increased the hardness values to 27 ± 3 HV and 28 ± 4 HV demonstrating the rises of 27% and 35%, respectively. Despite the fact that relative densities of the composites are decreasing by increasing the contents of GNPs, the hardness is still increasing. A similar observation

https://doi.org/10.1557/jmr.2017.111 Published online by Cambridge University Press

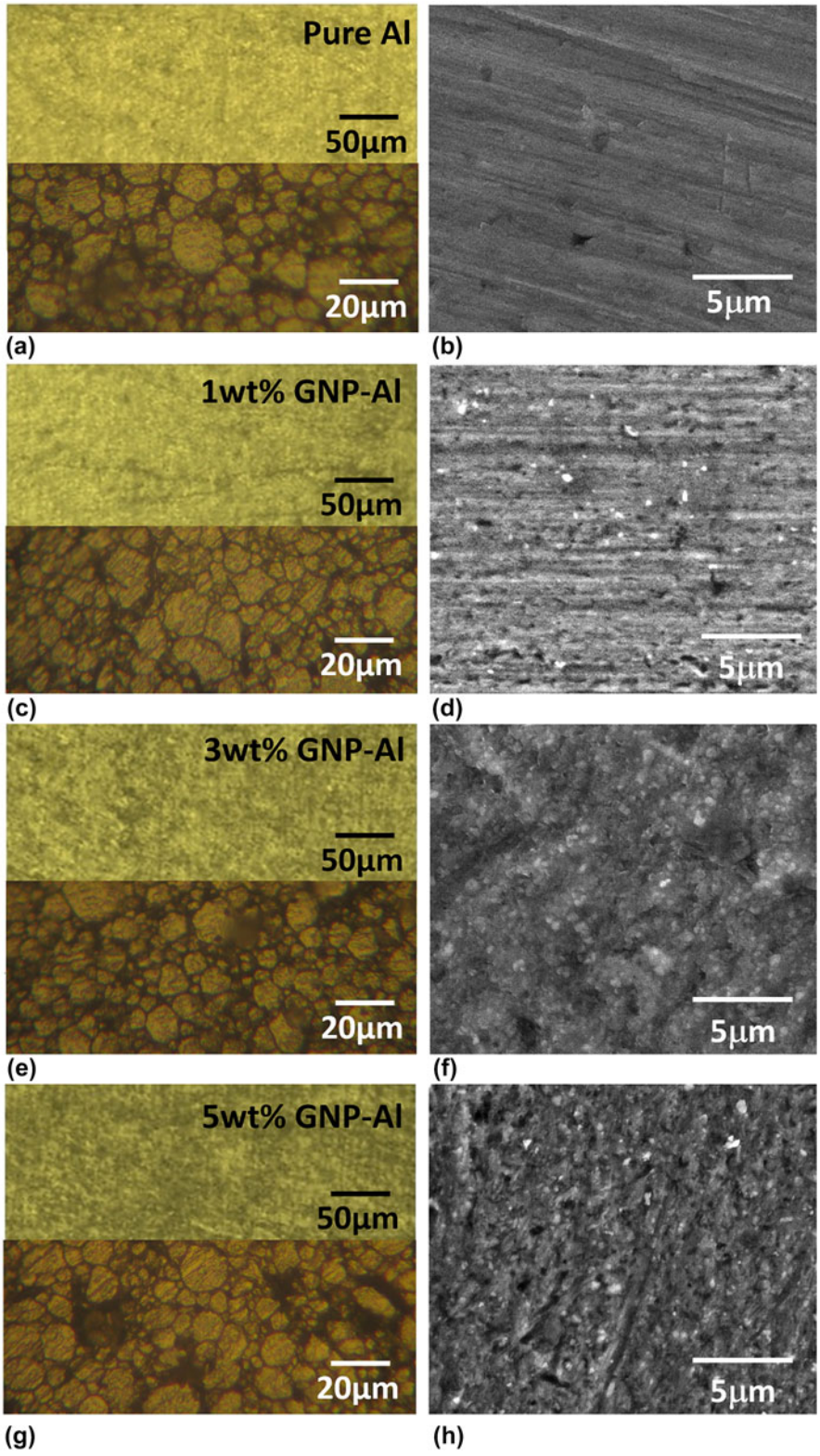


FIG. 5. Optical images of polished surfaces at 100× (upper halves) and etched surfaces at 400× magnifications (lower halves) of (a) pure aluminum, (c) 1 wt% GNP–Al, (e) 3 wt% GNP–Al, and (g) 5 wt% GNP–Al. SEM micrographs of polished surfaces of (b) pure aluminum, (d) 1 wt% GNP–Al, (f) 3 wt% GNP–Al, and (h) 5 wt% GNP–Al composites.

https://doi.org/10.1557/jmr.2017.111 Published online by Cambridge University Press

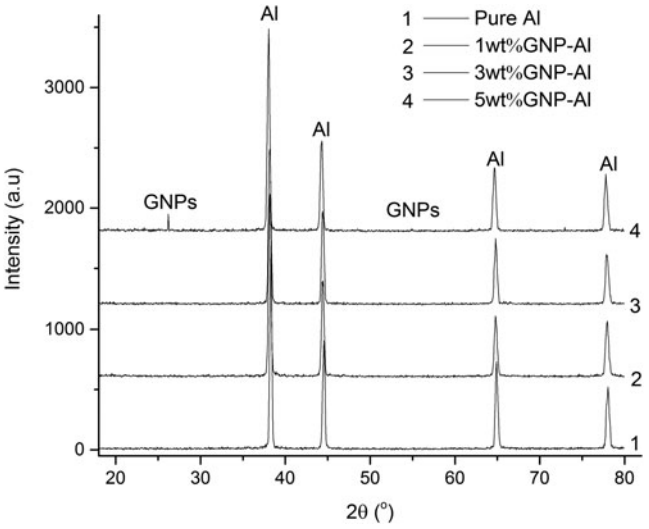


FIG. 6. XRD plots of pure aluminum and aluminum matrix composites containing GNPs; the presence of GNPs was detected in composites containing 5 wt% GNPs.

TABLE I. Theoretical, experimental, and relative densities of pure aluminum and aluminum matrix composites containing GNPs.

Samples	Theoretical density (g/cm^3)	Experimental density (g/cm^3)	Relative density (%)
Pure Al	2.7	2.66 ± 0.3	98.6 ± 0.3
1 wt% GNP–Al	2.69	2.63 ± 0.4	97.4 ± 0.5
3 wt% GNP–Al	2.68	2.58 ± 0.2	96.2 ± 0.4
5 wt% GNP–Al	2.67	2.56 ± 0.3	95.8 ± 0.5

was noted elsewhere.[11] It can be inferred that 100% densification of the composites processed by pressure-assisted sintering techniques may show even better hardness values than that observed in the present investigation. The literature shows both increasing[17,23] and decreasing[25] trends in hardness values of GNP-AMCs. Contrary to continuous increase and decrease in hardness, initial rise followed by fall in hardness has also been observed.[21,24]

Increase in the hardness of composites is the direct indication of the increase in the strength of composites. The densification of composites and uniform dispersion of GNPs are the two main factors contributing to the enhancement of hardness. Insufficient densification and poor dispersion of GNPs lead to reduced hardness values. The reduction in grain size may be another factor but in the composites under investigation, no significant decrease in the grain size of the aluminum matrix was observed by incorporating GNPs and the composites retained the grain boundaries as that of original particle surfaces. The grain size as evaluated from Fig. 5 is ~10 μm and no significant change in grain size was observed in the presence of GNPs. Therefore, it can be concluded that the increase in hardness is mainly due to the uniform distribution of GNPs and densification. Another strengthening mechanism explained by researchers is the difference in coefficients of thermal expansion (CTE) of reinforcement and matrix.[26] This results in thermal mismatch leading to generation of stresses between reinforcement and matrix, thus directly influencing the hardness. Dislocation peening has also been reported in the literature due to thermal stresses.[27] Moreover, the formation of Al_4C_3 also decreases the hardness of composites, as observed in a study.[28] Similarly, the milling and sintering times have also found to affect the hardness values; an increase in the milling time and a decrease in the sintering time produce fine structures and thus increased hardness.[29] Finally, the increase in hardness can be obtained by applying secondary processing such as rolling, forging, or extrusion[30]; the effect cause from mechanical working.

F. Compressive strength

Figure 7(c) shows the compressive strength values of pure aluminum and composites. A similar increasing trend in compressive strength was observed as noted in hardness values. Pure aluminum showed the compressive strength value of 15 ± 5 MPa, which increased to 38 ± 3, 61 ± 5, and 82 ± 4.5 MPa by adding 1, 3, and 5 wt% GNPs showing the rises of 153, 307, and 433%, respectively. Like hardness, the literature shows both rising and falling trends in the compressive strength of composites.[11,17] The orientation of GNPs during the compressive test affects the strength of composites.[17] If GNPs are parallel to the applied load, these will buckle during compression and bend at an angle of 45°. The application of further load will rupture the GNPs resulting in a significant decrease in compressive properties. In contrast, if GNPs are aligned perpendicular to the applied load, these will not contribute to compressive strength. The multilayers in GNPs may also shear due to the presence of weak van der Waals forces between the layers.[31]

G. Flexural strength

Flexural strength values of pure aluminum and composites are shown in Fig. 7(d). It can be seen that the incorporation of GNPs in aluminum increased the flexural strength. Pure aluminum had a value of 60 ± 3 MPa, which increased to 120 ± 8 MPa, 200 ± 10 MPa, and 230 ± 11 MPa by adding 1 wt%, 3 wt%, and 5 wt% GNPs showing the rises of 100%, 233%, and 283%, respectively. In a different study, 47% increase in the flexural strength was noted by adding 1 wt% GNPs in aluminum alloy 6061[16]; increase in the strength was related to the increase in the ball milling time of composite powder.

H. Fractography

The fractured specimens after compression testing are shown in Figs. 8(a)–8(d). The compressive load on the specimens was normal to the direction of applied load

https://doi.org/10.1557/jmr.2017.111 Published online by Cambridge University Press

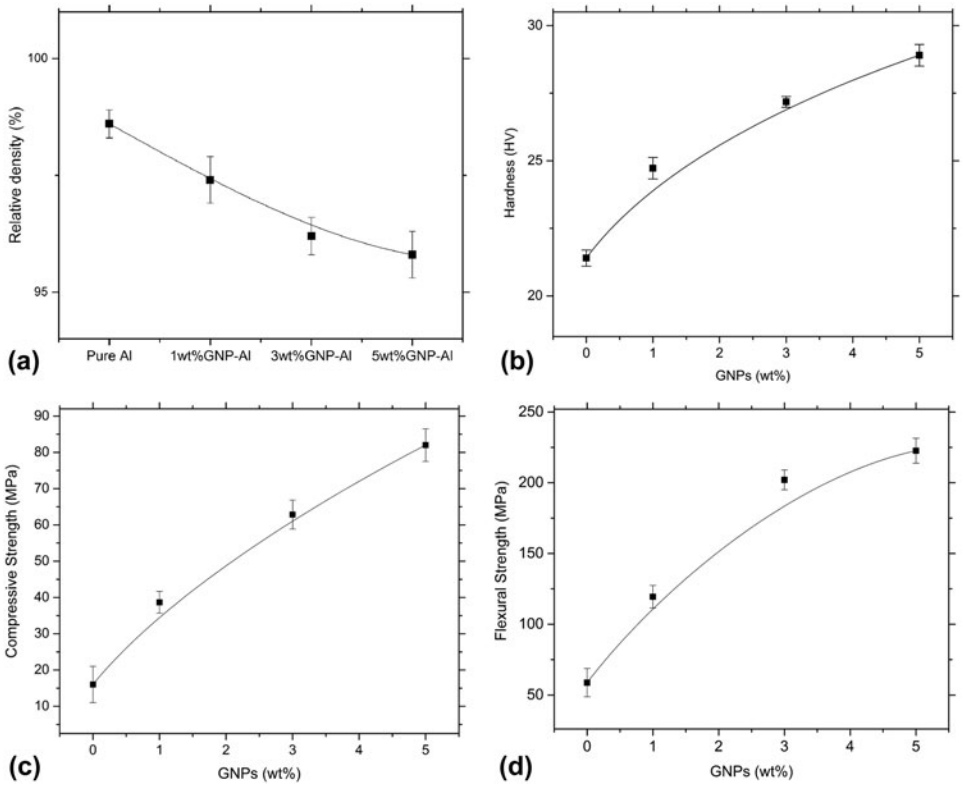


FIG. 7. (a) Relative densities, (b) hardness, (c) compressive strength, and (d) flexural strength values of pure aluminum and composites containing GNPs.

during composite green body preparation. Therefore, compressive load applied a tensile stress at a perpendicular direction and caused the fracture of specimens like the failure of specimens under diametral compression test.[32] Buckling in the specimens was observed especially in pure aluminum [Fig. 8(a)], which decreased with increasing contents of GNPs. In composite containing 5 wt%, no buckling was observed [Fig. 8(d)] and the specimen failed in a brittle manner. It can be inferred from the fracture specimens that the rising contents of GNPs reduced the ductility of aluminum and induced brittleness though the increase in strength was accompanied.

To further investigate the effect of GNPs on the fracture of composites, the fracture surfaces of the compression test specimens were observed under SEM to find the fracture morphology. The dimples were seen on the fracture surface of pure aluminum specimens, which were not completely spherical [Figs. 8(e) and 8(i)]. The morphology of these dimples is also different from those observed on the fracture surface of tensile specimens tested under tensile loading.[33] It can be expected that the fracture ran through the prior aluminum powder surface, cold compacted followed by densified through sintering. Small voids on the fracture surface are also visible, which may be due to the pull out of fine aluminum particles.

The fracture surface of composite containing 1 wt% GNPs did not show the presence of any dimples, which was also relatively smooth than pure aluminum specimen [Figs. 8(f) and 8(j)]. However, a different surface morphology comprising pultruded features was observed. These features may be sheared graphene layers attached with the aluminum matrix along the fracture surface. In composites, the graphene layers were incorporated along the surface of aluminum powder as well as embedded in the soft aluminum powders because aluminum powders deform plastically during ball milling[34] and GNPs were embedded in it. A good bonding between the fiber/matrix results in an increase in the strength of composites. As there was no chemical bonding in the present work, i.e., no formation of Al_4C_3, as evidenced by XRD, it can be assumed that a strong mechanical bonding came into effect due to the wrinkled nature of graphene, which actually increased the bonding strength at the GNP/Al interface. During the application of stress, load was transferred from aluminum to GNPs, which oriented themselves along the loading direction and after bearing a maximum load, either GNPs were pulled out of the matrix or these were sheared and thus separated while still sticking on the aluminum matrix, as evidenced in composites containing 3 wt% and 5 wt% GNPs in Figs. 8(g), 8(k), 8(h), and 8(l). The fracture of individual graphene

https://doi.org/10.1557/jmr.2017.111 Published online by Cambridge University Press

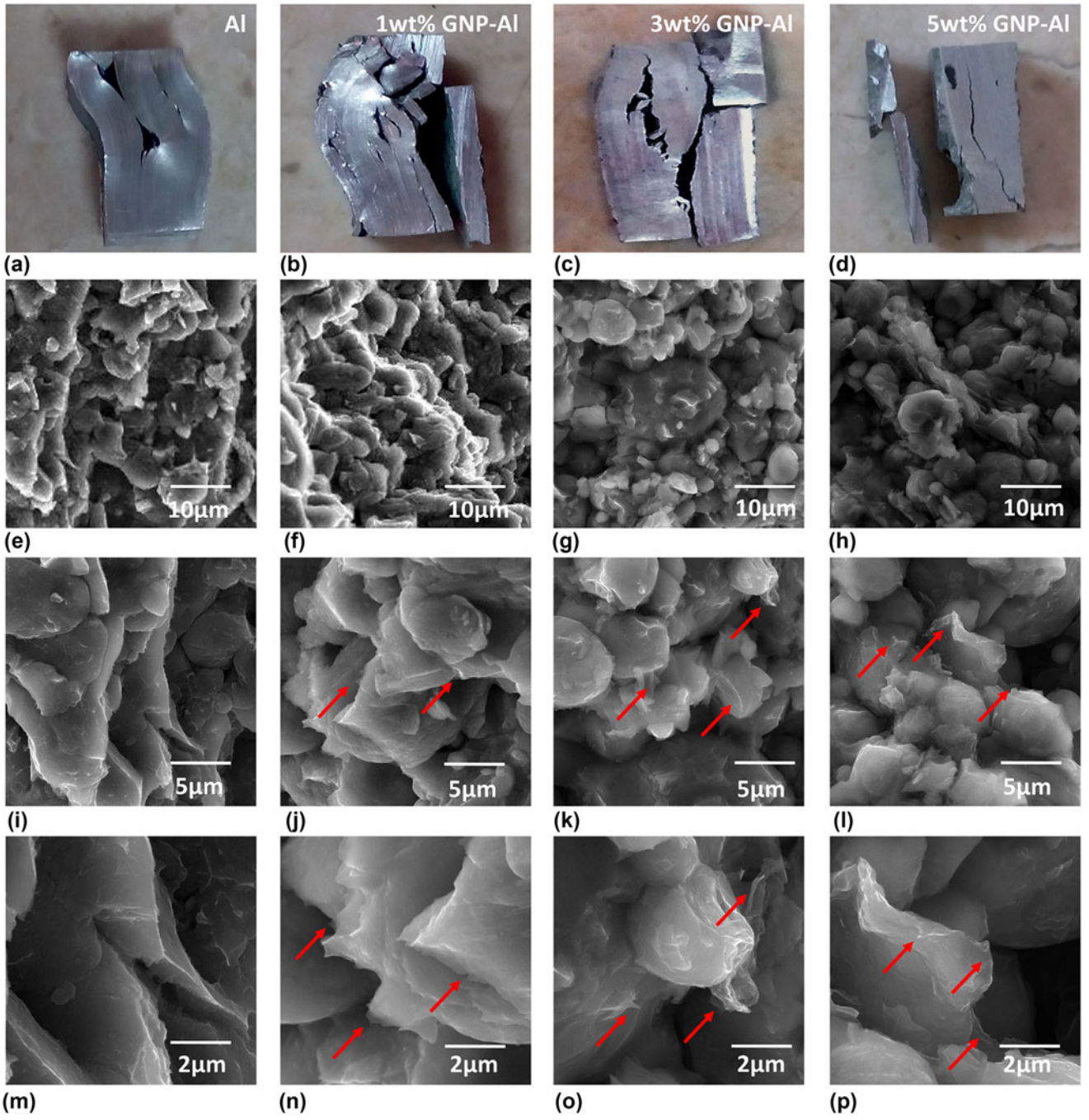


FIG. 8. Compression test specimens of (a) pure aluminum, (b) 1 wt% GNP–Al, (c) 3 wt% GNP–Al, and (d) 5 wt% GNP–Al composites after fracture. SEM micrographs of (e, i, and m) fractured surface of pure aluminum, (f, j, and n) fractured surface of 1 wt% GNP–Al, (g, k, and o) fractured surface of 3 wt% GNP–Al, and (h, l, and p) fracture surface of 5 wt% GNP–Al composite with increasing order of magnification.

layers may only be possible when the interfacial shear strength exceeds their tensile strength. In the present argument of the presence of a mechanical bond, it seems difficult to predict that individual graphene layers fractured during pull out. Nevertheless, shearing within GNPs may be possible.

To further understand the fracture morphology of the composites, SEM images at higher magnification were acquired [Figs. 8(m)–8(p)]. It is to be noted that the pointed surface morphology on the fracture surface of pure aluminum [Fig. 8(m)] changed into partially spherical morphology by incorporating 1 wt% GNPs in aluminum [Fig. 8(n)]. During the process of fracturing the pure aluminum specimen, pointed surfaces were created after considerable plastic deformation. However, after incorporating GNPs in aluminum, the fracture mode

https://doi.org/10.1557/jmr.2017.111 Published online by Cambridge University Press

was mainly dominated by GNPs and no such pointed morphology was observed. Instead, round surface features were observed due to the shearing of GNPs, which increased with the increase in the contents of GNPs [Figs. 8(o) and 8(p)]. The edges of nanometer thickness at the fracture composite specimen surfaces may be the pultruded graphene layers with attached aluminum matrix.

IV. CONCLUSIONS

Novel nanocomposites of pure aluminum containing GNPs were manufactured by powder metallurgy technique. Solution sonication and ball milling processes were used to prepare composite powders containing uniformly dispersed GNPs in loadings of 1, 3, and 5 wt%. The combination of uniaxial pressing and pressureless sintering was used for the densification of composite powders into compact composite bodies. Microstructural characterization through XRD confirmed the absence of any potential reaction between aluminum and GNPs thus avoiding the formation of Al_4C_3, while SEM images showed uniform dispersion of GNPs and the absence of their agglomerates. The increased mechanical properties of composites were found with rising contents of GNPs with the maximum improvements of 35%, 433%, and 283% in hardness, compression, and flexural strength in composites containing 5 wt% GNPs, respectively. The fracture morphology of composites changed from pure ductile in aluminum to brittle in composites due to increased strength. Pull out and shearing of GNPs were noticed during the fracture of composites with simultaneous restricted plastic deformation of aluminum matrix. The fracture morphology changed from matrix-dominant in pure aluminum to reinforcement-dominant in composites. A good combination of strength and ductility in GNP–Al composites can be attained for a specific application. GNP–Al composites are therefore potential candidates for futuristic demands of advanced materials for various structural applications in aerospace and automobile industries.

REFERENCES

1. X-H. Chen and H. Yan: Fabrication of nanosized Al_2O_3 reinforced aluminum matrix composites by subtype multifrequency ultrasonic vibration. *J. Mater. Res.* **30**, 2197 (2015).
2. S. Hao and J. Xie: Tensile properties and strengthening mechanisms of SiC p-reinforced aluminum matrix composites as a function of relative particle size ratio. *J. Mater. Res.* **28**, 2047 (2013).
3. M. Hanabe and P. Aswath: Al_2O_3/Al particle-reinforced aluminum matrix composite by displacement reaction. *J. Mater. Res.* **11**, 1562 (1996).
4. H.B. Michael Rajan, S. Ramabalan, I. Dinaharan, and S.J. Vijay: Synthesis and characterization of in situ formed titanium diboride particulate reinforced AA7075 aluminum alloy cast composites. *Mater. Des.* **44**, 438 (2013).
5. D. Lloyd: Particle reinforced aluminium and magnesium matrix composites. *Int. Mater. Rev.* **39**, 1 (1994).
6. K. Shirvanimoghaddam, S.U. Hamim, M. Karbalaei Akbari, S.M. Fakhrhoseini, H. Khayyam, A.H. Pakseresht, E. Ghasali, M. Zabet, K.S. Munir, S. Jia, J.P. Davim, and M. Naebe: Carbon fiber reinforced metal matrix composites: Fabrication processes and properties. *Composites, Part A* **92**, 70 (2017).
7. S. Rawal: Metal–matrix composites for space applications. *JOM* **53**, 14 (2001).
8. S.R. Bakshi, D. Lahiri, and A. Agarwal: Carbon nanotube reinforced metal matrix composites—A review. *Int. Mater. Rev.* **55**, 41 (2010).
9. X. Gao, H. Yue, E. Guo, H. Zhang, X. Lin, L. Yao, and B. Wang: Preparation and tensile properties of homogeneously dispersed graphene reinforced aluminum matrix composites. *Mater. Des.* **94**, 54 (2016).
10. Y. Sun, Y. Lyu, A. Jiang, and J. Zhao: Fabrication and characterization of aluminum matrix fly ash cenosphere composites using different stir casting routes. *J. Mater. Res.* **29**, 260 (2014).
11. F.H. Latief, E-S.M. Sherif, A.A. Almajid, and H. Junaedi: Fabrication of exfoliated graphite nanoplatelets-reinforced aluminum composites and evaluating their mechanical properties and corrosion behavior. *J. Anal. Appl. Pyrolysis* **92**, 485 (2011).
12. S.J. Yan, S.L. Dai, X.Y. Zhang, C. Yang, Q.H. Hong, J.Z. Chen, and Z.M. Lin: Investigating aluminum alloy reinforced by graphene nanoflakes. *Mater. Sci. Eng., A* **612**, 440 (2014).
13. W-m. Tian, S-m. Li, B. Wang, X. Chen, J-h. Liu, and M. Yu: Graphene-reinforced aluminum matrix composites prepared by spark plasma sintering. *Int. J. Miner., Metall. Mater.* **23**, 723 (2016).
14. I. Ahmad, M. Islam, T. Subhani, and Y. Zhu: Characterization of GNP-containing Al_2O_3 nanocomposites fabricated via high frequency-induction heat sintering route. *J. Mater. Eng. Perform.* **24**, 4236 (2015).
15. I. Ahmad, M. Islam, H.S. Abdo, T. Subhani, K.A. Khalil, A.A. Almajid, B. Yazdani, and Y. Zhu: Toughening mechanisms and mechanical properties of graphene nanosheet-reinforced alumina. *Mater. Des.* **88**, 1234 (2015).
16. M. Bastwros, G-Y. Kim, C. Zhu, K. Zhang, S. Wang, X. Tang, and X. Wang: Effect of ball milling on graphene reinforced Al6061 composite fabricated by semi-solid sintering. *Composites, Part B* **60**, 111 (2014).
17. M. Rashad, F. Pan, A. Tang, and M. Asif: Effect of graphene nanoplatelets addition on mechanical properties of pure aluminum using a semi-powder method. *Prog. Nat. Sci.: Mater. Int.* **24**, 101 (2014).
18. H. Zhang, C. Xu, W. Xiao, K. Ameyama, and C. Ma: Enhanced mechanical properties of Al5083 alloy with graphene nanoplates prepared by ball milling and hot extrusion. *Mater. Sci. Eng., A* **658**, 8 (2016).
19. L.A. Yolshina, R.V. Muradymov, I.V. Korsun, G.A. Yakovlev, and S.V. Smirnov: Novel aluminum–graphene and aluminum–graphite metallic composite materials: Synthesis and properties. *J. Alloys Compd.* **663**, 449 (2016).
20. M. Ipekoglu, A. Nekouyan, O. Albayrak, and S. Altintas: Mechanical characterization of B_4C reinforced aluminum matrix composites produced by squeeze casting. *J. Mater. Res.* **1**, 599 (2017).
21. A. Ghazaly, B. Seif, and H.G. Salem: Mechanical and tribological properties of AA2124-graphene self lubricating nanocomposite. In *Light Metals 2013* (John Wiley & Sons, Inc., Hoboken, 2013); p. 411.
22. K.V. Zakharchenko, F. Annalisa, J.H. Los, and M.I. Katsnelson: Melting of graphene: From two to one dimension. *J. Phys.: Condens. Matter* **23**, 202202 (2011).
23. J. Liu, U. Khan, J. Coleman, B. Fernandez, P. Rodriguez, S. Naher, and D. Brabazon: Graphene oxide and graphene

https://doi.org/10.1557/jmr.2017.111 Published online by Cambridge University Press

nanosheet reinforced aluminium matrix composites: Powder synthesis and prepared composite characteristics. *Mater. Des.* **94**, 87 (2016).
24. S.N. Alam and L. Kumar: Mechanical properties of aluminium based metal matrix composites reinforced with graphite nanoplatelets. *Mater. Sci. Eng., A* **667**, 16 (2016).
25. M. Tabandeh-Khorshid, E. Omrani, P.L. Menezes, and P.K. Rohatgi: Tribological performance of self-lubricating aluminum matrix nanocomposites: Role of graphene nanoplatelets. *Eng. Sci. Technol., Int. J.* **19**, 463 (2016).
26. V. Sharma, U. Prakash, and B.V.M. Kumar: Surface composites by friction stir processing: A review. *J. Mater. Process. Technol.* **224**, 117 (2015).
27. Z. Hu, G. Tong, D. Lin, C. Chen, H. Guo, J. Xu, and L. Zhou: Graphene-reinforced metal matrix nanocomposites–A review. *Mater. Sci. Technol.* **32**, 930 (2016).
28. S.F. Bartolucci, J. Paras, M.A. Rafiee, J. Rafiee, S. Lee, D. Kapoor, and N. Koratkar: Graphene–aluminum nanocomposites. *Mater. Sci. Eng., A* **528**, 7933 (2011).
29. R. Pérez-Bustamante, D. Bolaños-Morales, J. Bonilla-Martínez, I. Estrada-Guel, and R. Martínez-Sánchez: Microstructural and hardness behavior of graphene-nanoplatelets/aluminum composites synthesized by mechanical alloying. *J. Alloys Compd.* **615** (Suppl. 1), S578 (2014).
30. Z. Li, G. Fan, Q. Guo, Z. Li, Y. Su, and D. Zhang: Synergistic strengthening effect of graphene–carbon nanotube hybrid structure in aluminum matrix composites. *Carbon* **95**, 419 (2015).
31. M. Rashad, F. Pan, A. Tang, M. Asif, S. Hussain, J. Gou, and J. Mao: Improved strength and ductility of magnesium with addition of aluminum and graphene nanoplatelets (Al + GNPs) using semi powder metallurgy method. *J. Ind. Eng. Chem.* **23**, 243 (2015).
32. F. Bonollo, B. Molinas, I. Tangerini, and A. Zambon: Diametral compression testing of metal matrix composites. *Mater. Sci. Technol.* **10**, 558 (1994).
33. M. Karbalaei Akbari, H.R. Baharvandi, and K. Shirvanimoghaddam: Tensile and fracture behavior of nano/micro TiB_2 particle reinforced casting A356 aluminum alloy composites. *Mater. Des.* **66**(Part A), 150 (2015).
34. S.E. Shin and D.H. Bae: Deformation behavior of aluminum alloy matrix composites reinforced with few-layer graphene. *Composites, Part A* **78**, 42 (2015).

https://doi.org/10.1557/jmr.2017.111 Published online by Cambridge University Press